Journal of Hazardous Materials 447 (2023) 130772

Contents lists available at ScienceDirect

Journal of Hazardous Materials

journal homepage: www.elsevier.com/locate/jhazmat

Efficient lead immobilization by bio-beads containing *Pseudomonas rhodesiae* and bone char

Junpeng Li [a,b], Rui Bai [a,b], Wei Chen [a,c], Chongyuan Ren [a,b], Fan Yang [a,b], Xiaochun Tian [a], Xiaofeng Xiao [a,b], Feng Zhao [a,*]

[a] CAS Key Laboratory of Urban Pollutant Conversion, Institute of Urban Environment, Chinese Academy of Sciences, Xiamen 361021, China
[b] University of Chinese Academy of Sciences, Beijing 100049, China
[c] College of Life Sciences, Fujian Agriculture and Forestry University, Fuzhou 350002, China

HIGHLIGHTS

- Bio-beads containing *Pseudomonas rhodesiae* HP-7 and bone char were prepared.
- Bone char turned into effective Pb remedial material in the presence of HP-7 strain.
- Acid soluble fraction Pb in the soil was reduced by 34 % after remediation.
- Bio-beads show stability during one-month Pb contamination remediation.

GRAPHICAL ABSTRACT

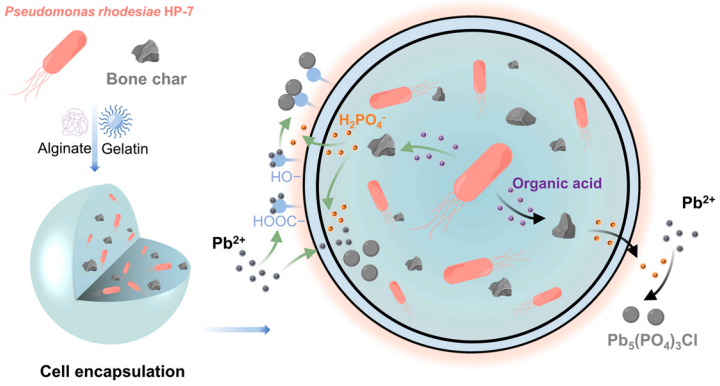

ARTICLE INFO

Editor: Dr. R. Debora

Keywords:
Bioremediation
Lead
Encapsulation
Phosphate-solubilizing bacteria
Bone char

ABSTRACT

Mineralization of lead ions (Pb^{2+}) to pyromorphite using phosphorus-containing materials is an effective way to remediate lead (Pb) contamination. Bone char is rich in phosphorus, but its immobilization of Pb^{2+} is limited by poor phosphate release. To utilize the phosphorus in bone char and provide a suitable growth environment for phosphate-solubilizing bacteria, bone char and *Pseudomonas rhodesiae* HP-7 were encapsulated into bio-beads, and the immobilization performance and mechanism of Pb in solution and soil by bio-beads were investigated. The results showed that 137 mg/g of phosphorus was released from bone char in the presence of the HP-7 strain. Pb^{2+} removal efficiency reached 100 % with an initial Pb^{2+} concentration of 1 mM, bone char content of 6 g/L, and bio-bead dosage of 1 %. Most Pb^{2+} was immobilized on the surface of the bio-beads as $Pb_5(PO_4)_3Cl$. The soil remediation experiments showed a 34 % reduction in the acid-soluble fraction of Pb. The bio-beads showed good stability in long-term (30 d) soil remediation. The present study shows that bone char can be turned into an efficient Pb immobilization material in the presence of phosphate-solubilizing bacteria. Thus, bio-beads are expected to be used in the remediation of Pb-contaminated environments.

* Corresponding author.
E-mail address: fzhao@iue.ac.cn (F. Zhao).

https://doi.org/10.1016/j.jhazmat.2023.130772
Received 10 November 2022; Received in revised form 23 December 2022; Accepted 9 January 2023
Available online 13 January 2023

Environmental implication

Lead (Pb) pollution is a serious environmental problem. The mineralization of lead ions to pyromorphite is considered an effective remediation method. The bio-beads containing bone char and phosphate-solubilizing bacteria HP-7 developed in this work can be used for the efficient immobilization of lead in solution and soil. The bio-beads showed good stability in long-term soil remediation, and the strain within the bio-beads could grow. This study provides a method to achieve resourceful use of waste animal bones and remediation of lead contamination.

Data availability

No data was used for the research described in the article.

1. Introduction

Lead (Pb) pollution has become one of the most serious environmental problems endangering human and animal health [1]. Mineralization of highly bioavailable lead ions (Pb^{2+}) to low-bioavailable pyromorphite ($Pb_5(PO_4)_3X$, X = F, Cl, Br, or OH, $Ksp = 10^{-71.6} \sim -84.4$) is an effective form of remediation [2]. Phosphate is required for pyromorphite formation [3]. Phosphate rock, tricalcium phosphate, hydroxyapatite, fluorapatite, and other phosphate minerals have been used for the mineralization of Pb^{2+} [4-8]. However, phosphorus (P) is an indispensable element for agricultural production, and the rapid depletion of phosphate minerals has led to a rapid scarcity of P resources [9,10]. Therefore, it is important to find safe, low-cost, and readily available materials containing P to remediate Pb-contaminated environments [11].

Biochar is produced from a variety of plants or manure materials under anoxic conditions. The carbon content of biochar is usually greater than 70 %, whereas the P content is usually less than 1 % (except for biochar of manure origin, which contains 2.6 %−13.5 % as P_2O_5) [12]. Owing to its rich pore structure and large specific surface area, biochar can be used as a carrier in functional composites [13]. Wu et al. [14] synthesized a hydroxyapatite-tailored hierarchical porous biochar for the adsorption and immobilization of Cd(II) and Pb(II) in water and soil. Li et al. [15] proposed a molybdenum trioxide (MoO_3)-engineered biochar as an adsorbent for Pb^{2+} removal. Ren et al. [16] prepared a Ca$(H_2PO_4)_2$-engineered swine manure biochar for the remediation of Pb- and cadmium-contaminated soils. Bone char is a product of animal bone pyrolysis under anoxic conditions and consists mainly of hydroxyapatite (70 %−76 %), calcium carbonate (7 %−9 %), and amorphous carbon (9 %−11 %) [17]. More than 20 million tons of all types of livestock and poultry bones are produced annually in China [18]. However, most animal bones are not rationally used. This not only results in a waste of P resources but also causes environmental pollution owing to bone decay. Hydroxyapatite, the main component of bone char, is an inorganic material with good adsorption properties that can remove metal ions from solution by adsorption [18]. Liu et al. [19] prepared amino-modified pig bone char for the adsorption of Pb(II) and Cu(II), with adsorption capacities of 120 and 30 mg/g, respectively. Xiao et al. [20] prepared bovine bone char using a ball milling technique with adsorption capacities of 165.8, 287.6, and 558.9 mg/g for Cd(II), Cu(II), and Pb(II), respectively. The mineralization of Pb is preferable for sorption in soil remediation [21]. Soluble phosphate is essential for the mineralization of Pb^{2+}. Although bone char contains up to 17 % P, its release is difficult [11]. Phosphate-solubilizing bacteria promote the dissolution of phosphate minerals such as tricalcium phosphate and fluorapatite [5,6]. In our previous study, a phosphate-solubilizing bacterium, *Pseudomonas rhodesiae* HP-7, was isolated and was able to dissolve 84.5 % of P from synthetic hydroxyapatite [4]. However, there are few reports on phosphate-solubilizing bacteria that promote P release from bone char [22]. Whether phosphate-solubilizing bacteria can release P from the bone char under Pb stress remains unknown.

Contaminant toxicity and competition from indigenous microorganisms can inhibit the growth of phosphate-solubilizing bacteria in the environment. To address this issue, researchers have considered encapsulating bacteria or providing bacteria with habitat carriers to counteract inhibitory effects. For example, Zhang et al. [8] encapsulated the phosphate-solubilizing bacteria *Leclercia adecarboxylata* L15 and $Ca_3(PO_4)_2$ in capsules for remediation of lead-contaminated sediments. Teng et al. [23] encapsulated *L. adecarboxylata* L15, biochar, and nano-zero-valent iron in bio-beads, and investigated the solubilization ability of $Ca_3(PO_4)_2$ and the immobilization performance of Pb^{2+}. The results showed that the bio-beads had higher P solubilization and Pb immobilization capacity than free bacteria. Tu et al. [24] found that biochar with a porous structure could serve as an ideal habitat for microorganisms, thereby improving the effectiveness of pig manure composting. Although bone char has a higher P content than biochar, it does not provide a habitat for microorganisms because of its small specific surface area and pore structure [11]. To use the abundant P in bone char and provide a suitable environment for the growth of phosphate-solubilizing bacteria, this study used sodium alginate and gelatin to encapsulate both bone char and the phosphate-solubilizing HP-7 bacteria in bio-beads. Sodium alginate is a polysaccharide extracted from algae or bacteria that can be combined with divalent cations to form a hydrogel with a certain mechanical strength. It is commonly used for cellular encapsulation and controlled release of drugs [25]. Gelatin is a product of collagen hydrolysis, and its composition is similar to that of the natural extracellular matrix. It supports cell adhesion and proliferation and is commonly used in 3D cell culture; however, its mechanical strength is low [26]. The combination of alginate and gelatin not only mimics the amino acid and polysaccharide components of the extracellular matrix but also has a certain mechanical strength, which facilitates the construction of suitable bacterial encapsulation materials.

The aims of this study were 1) to construct bacterial encapsulation materials by optimizing the ratio of sodium alginate to gelatin; 2) to study the ability of the HP-7 strain to release P from bone char; and 3) to investigate the mechanism of Pb^{2+} immobilization and long-term stability of bio-beads encapsulated with phosphate-solubilizing bacteria and bone char.

2. Materials and methods

2.1. Chemicals

Sodium alginate was purchased from Aladdin Reagent Company (Shanghai, China). Gelatin, calcium chloride, and other reagents were purchased from Sinopharm (Shanghai, China). Bovine bone granules were purchased from Xingtai (Hebei Province, China). The nitric acid, hydrochloric acid, and hydrofluoric acid used in this study were of superior purity, and all other reagents were of analytical purity.

2.2. Preparation of bone char

The bovine bone particles were crushed using a pulverizer and sieved to obtain small particles with diameters less than 0.45 mm. The particles were placed in a ceramic crucible and charred in a tube furnace under anoxic conditions [20]. High-purity nitrogen (99.999 %) was continuously introduced into the tube furnace at a rate of 0.1 NL/min during the charring process. The charring temperature was between 200 °C and 600 °C (100 °C intervals), with a heating rate of 5 °C/min and charring time of 5 h. After charring, the bone char was sieved again to obtain 0.075 mm < d < 0.15 mm for encapsulation.

2.3. Culture of P. rhodesiae

Pseudomonas rhodesiae HP-7 was isolated from Pb-contaminated soil [4]. The conserved *P. rhodesiae* was activated in beef extract-peptone liquid medium (BP medium: 3 g/L beef extract, 10 g/L peptone, and 5 g/L NaCl). The pH of the medium was adjusted to 7.0. Activated *P. rhodesiae* were re-transformed into BP medium at 30 °C and 150 rpm for 15 h. The resulting broth was centrifuged at 3000 × *g* for 5 min to obtain bacteria. The bacteria were washed three times using mineral medium (5 g/L $NaNO_3$, 0.2 g/L KCl, and 0.1 g/L $(NH_4)_2SO_4$, pH 6.5), resuspended, and adjusted to an of OD_{600} = 1.0. This suspension was used to encapsulate bacteria.

2.4. Preparation of bio-beads

Preparation of beads was performed as previously described with modifications [27]. Specifically, gelatin (1 g) and sodium alginate (0.25 g, 0.333 g, 0.5 g, 1 g, 2 g, 3 g, or 4 g) were dissolved in 100 mL of mineral medium and stirred at 80 °C in a water bath until completely dissolved. The ratios of gelatin to alginate in the solution were 4:1, 3:1, 2:1, 1:1, 1:2, 1:3, and 1:4. After the solution had cooled to room temperature (25–30 °C), it was transferred to a 10 mL syringe and added dropwise to a 2 % $CaCl_2$ solution using a syringe pump at a flow rate of 0.95 mL/min. After 3 h of curing, the beads were washed thrice with the mineral medium.

Based on the morphology and mechanical strength of the resulting beads, an optimum ratio of seven was selected for encapsulation of the HP-7 strain and bone char. The process of encapsulating the HP-7 strain and bone char was as follows. Briefly, 100 mL of bacterial solution at OD_{600} = 1 was centrifuged (3000×*g*, 5 min), resuspended in 10 mL of mineral medium, and subsequently added to 90 mL of cooled gelatin and alginate solution with a certain mass of bone char. After thorough mixing, the mixture was transferred to a 10 mL syringe following the same procedure. Bio-beads containing only bacteria and beads containing only bone char were prepared in the same manner. The resulting beads were used for subsequent experiments.

2.5. Growth of the HP-7 strain in bio-beads and dissolution of phosphate in bone char

To show that the HP-7 strain could grow properly inside the bio-beads, the following experiments were performed. Low levels of bacteria (5 mL OD_{600} = 1) were encapsulated inside the bio-beads, which were placed in 96-well plates. Each well contained one bio-bead, and 200 μL of BP medium was added to each well. The 96-well plates were then incubated at 30 °C. At regular intervals, the bio-beads were removed, the center of the bio-beads was sectioned and stained with STYO9 (Thermo Fisher, LIVE/DEAD BacLight Bacterial Viability Kits), and the growth of the bacteria was observed under a fluorescent microscope (green fluorescence). Bio-beads containing the HP-7 strain, beads containing bone char, and bio-beads containing both the HP-7 strain and bone char were used for phosphate dissolution experiments. The dissolution experiments were carried out in 50 mL of a defined medium (DM medium) (10 g/L glucose, 5 g/L $NaNO_3$, 0.1 g/L $MgCl_2{\cdot}H_2O$, 0.2 g/L KCl, and 0.1 g/L $(NH_4)_2SO_4$). The pH was adjusted to 6.5 and then autoclaved at 121 °C for 20 min. The carbon source, glucose, was sterilized separately at 115 °C for 15 min and then added to the DM medium at a final concentration of 10 g/L. Three parallel experiments were performed for each experimental group. Approximately 3 mL of culture solution was collected at 0, 6, 12, 24, 48, and 72 h. The solutions were filtered through a 0.22 μm membrane and the pH was determined using a pH meter (UB-7, Denver, USA). The dissolved P content was determined using inductively coupled plasma optical emission spectrometry (ICP-OES, 7000 DV, PerkinElmer, USA).

2.6. Pb^{2+} removal

Pb^{2+} removal experiments were carried out in 200 mL conical flasks containing 50 mL of DM medium. Pb^{2+} mother liquor (10 g/L) was obtained by dissolving 1.6 g of $Pb(NO_3)_2$ in 100 mL of ultrapure water. The corresponding concentration of Pb^{2+} solution was obtained by pipetting a volume of Pb^{2+} mother liquor into the DM medium. Batch experiments were carried out to compare Pb^{2+} removal performance: (1) control experiment, (2) free bacteria, (3) bio-beads containing the HP-7 strain, (4) beads containing bone char, and (5) bio-beads containing both bone char and the HP-7 strain. The effects of bone char content (3, 4, 5, 6, and 7 g/L), bio-bead dosage (0.5 %, 0.8 %, 1 %, 1.2 %, and 1.5 %), and initial Pb^{2+} concentration (10.3, 103.5, 207, 310.5, 414, and 621 mg/L) on Pb^{2+} removal were also investigated. Three parallel experiments were performed for each experimental group. The conical flasks were incubated at 30 °C for 3 d at 150 rpm. After incubation, the supernatant was filtered through a 0.22 μm membrane, the pH was determined, and the dissolved Pb^{2+} concentration was measured using ICP-OES. The amount of P remaining in the solution was determined using the molybdenum blue colorimetric method (soil quality determination of available P-sodium hydrogen carbonate solution- Mo-Sb anti spectrophotometric method HJ 704–2014).

Pb^{2+} removal efficiency in solution was calculated according to the following formula:

$$\boldsymbol{Pb^{2+}removal\ \ efficiency} = \frac{\boldsymbol{C_0 - C}}{\boldsymbol{C_0}} \times \mathbf{100}\%$$

where C_o and C are the initial and final concentrations of Pb^{2+}, respectively (mg/L).

2.7. Lead-contaminated soil remediation

Lead-contaminated soil was collected from a smelter in Zhuzhou, Hunan Province, China. The total Pb content in the soil was 505 mg/kg, and the pH of the soil was 8.0. According to the Soil Environmental Quality Risk Control Standard for Soil Contamination of Development Land (GB 36600-2018), the soil was polluted by Pb (the minimum limit of total Pb is 400 mg/kg). After air-drying, grinding, and sieving (100-mesh), the soil sample was used for remediation experiments, which were carried out in 200 mL conical flasks after mixing 50 mL of DM medium and 5 g of soil [8]. To evaluate the remediation effect of bio-beads on lead-contaminated soil, five groups of experiments were conducted: (1) control experiment, (2) free bacteria (2 mL of bacterial solution with an OD_{600} of 1 was added to 50 mL of soil solution), (3) bio-beads containing the HP-7 strain (30 g/L), (4) beads containing bone char (30 g/L), and (5) bio-beads containing the HP-7 strain and bone char (30 g/L). The conical flasks were shaken at 30 °C for 30 days. After remediation, 10 mL of the soil solution was freeze-dried, and various fractions of Pb were extracted using a modified Community Bureau of Reference (BCR) sequential extraction method (Soil and sediment-Sequential extraction procedure of speciation of 13 trace elements GB/T 25282-2010). The Pb^{2+} concentrations in the extracts were determined using an inductively coupled plasma mass spectrometer (ICP-MS, Agilent 7500cx, USA).

2.8. Bead characterization

The beads were quickly washed thrice with 0.9 % NaCl solution, twice with ultrapure water, frozen overnight at −20 °C in a refrigerator, and subsequently dried using a freeze dryer. The dried beads were cut from the center using a razor blade and the resulting samples were observed using scanning electron microscopy (SEM, S-4800, Hitachi, Japan) for morphology evaluation. The dried beads were crushed, and the crystal structure of the material was determined using X-ray diffraction (XRD, X′ Pert Pro, PANalytical, Netherlands). Infrared

samples of alginate and gelatin were obtained by Ca^{2+} cross-linking into the films. The thin films were directly characterized using Fourier transform infrared spectroscopy (FT-IR, iS10, Thermoelectric Corporation, USA). The HP-7 strain (OD_{600} = 0.5, 50 mg/L Pb^{2+}, 12 h incubation) and bone char (0.05 g bone char, 300 mg/L Pb^{2+}, 12 h incubation) were characterized using FT-IR after pressing with KBr. The activity of bacteria inside the bio-beads was observed using fluorescence microscopy (Axio Imager A1, Zeiss, Germany) and laser confocal microscopy (LSM710, Zeiss, Germany). The center of the bio-beads was sectioned (thickness of approximately 100 μm) and subsequently stained with STYO9/PI for 20 min to visualize dead or live bacteria under a fluorescence microscope. After staining the bio-beads with STYO9/PI, the 3D distribution and activity of bacteria in the bio-beads were observed directly using laser confocal microscopy.

3. Results and discussion

3.1. Optimization of the alginate-to-gelatin ratio

The appearance and morphology of the beads produced using the seven ratios of gelatin-to-alginate are shown in Fig. S1. At ratios of 4:1 to 1:2, the beads were spherical in shape; when the ratio was reduced to 1:3 and 1:4, the beads showed trailing. This resulted from a gradual increase in viscosity of the mixed solution. The inset shows the cross sections of the beads in the seven ratios. When the ratio was 4:1 and 3:1, the mechanical strength of the beads was low and the spherical shape of the beads could not be maintained after drying and cutting off the faces; when the ratio was 1:2, the beads not only maintained their spherical shape but also showed a regular three-dimensional structure within, which not only facilitated the flow of nutrients but also the growth of bacteria within the bead (Fig. 1). When the ratio increased to 1:3 and 1:4, the beads were tadpole-shaped and showed an internal three-dimensional structure. The ratio of gelatin to alginate was chosen to be 1:2 for the encapsulation of the HP-7 strain and bone char, based on a combination of bead appearance, mechanical strength, and internal morphology.

3.2. Growth of the HP-7 strain in bio-beads

To determine whether the HP-7 strain encapsulated in the bio-beads could grow, the bio-beads were sectioned and stained, and the growth of the strain was observed under a fluorescence microscope (Fig. 2). At 0 h (Fig. 2a), only a few isolated strains were observed; after 24 h of incubation (Fig. 2b–d), the individual strain gradually grew into colonies consisting of multiple strains, with an increasing number of strains in the colonies. This result indicates that the bio-beads made from alginate and gelatin were biocompatible, and that the HP-7 strain encapsulated inside the bio-beads could grow.

3.3. P release from bone char in bio-beads

Bone char is a product of pyrolysis of waste animal bones under anoxic conditions [20]. It contains 10 % C and is rich in hydroxyapatite, an inorganic material with good adsorption properties for the removal of heavy metal ions [18]. However, the low solubility of hydroxyapatite limits the mineralization of Pb^{2+} [28]. Our previous study found that the HP-7 strain metabolized glucose to produce acetic acid, butyric acid, and isobutyric acid, and that these organic acids dissolved hydroxyapatite, thereby releasing soluble P [4]. The ability of the free HP-7 strain to release P from bone char at different pyrolysis temperatures is shown in Fig. S2. After 120 h of incubation, the bone char pyrolyzed at 500 °C in the presence of the HP-7 strain released the most soluble P, reaching 275 mg/L (137 mg P/g bone char). Tang et al. [22] investigated the P release properties of bone char obtained by pyrolysis of a porcine bone source at 100–300 °C in the presence of *Enterobacter spp*. The results showed that bone char pyrolyzed at 100 °C released the most soluble P at 77.37 mg/L (19.3 mg P/g bone char). Chen et al. [21] found that rice husk- and sludge-derived biochar released 122.1 mg/L (2.4 mg P/g biochar) and 84.3 mg/L (1.7 mg P/g biochar), respectively, of P under the action of *Enterobacter spp*. In the present study, the release of P from bone char in the presence of the HP-7 strain was much higher than that reported in previous studies. Comparing the results of this study with those of previous studies, the P content released by bone char under the action of phosphate-solubilizing bacteria was approximately 100 times higher than that of biochar. After pyrolysis, waste animal bones can be transformed into valuable P resources under the action of phosphate-solubilizing bacteria.

To confirm whether the HP-7 strain encapsulated inside the bio-beads still had the ability to release P, this study investigated the P-dissolving ability of the HP-7 strain by encapsulating it and bone char pyrolyzed at 500 °C inside the bio-beads, and the results are shown in Fig. 3. As shown in Fig. 3a, the pH gradually increased from 5.7 to 6.7 in the group of beads encapsulated with only bone char owing to its alkaline nature. The pH values of the groups encapsulating only the HP-7 strain and both the HP-7 strain and bone char decreased from 5.7 to 4.5 and 4.4, respectively, indicating that the HP-7 strain encapsulated inside the bio-beads could still metabolize glucose normally and secrete organic acids. As shown in Fig. 3b, dissolved P was released only in the group that encapsulated both bone char and HP-7 strain. The amount of dissolved P reached 41.9 mg/L after 72 h. This indicated that the HP-7

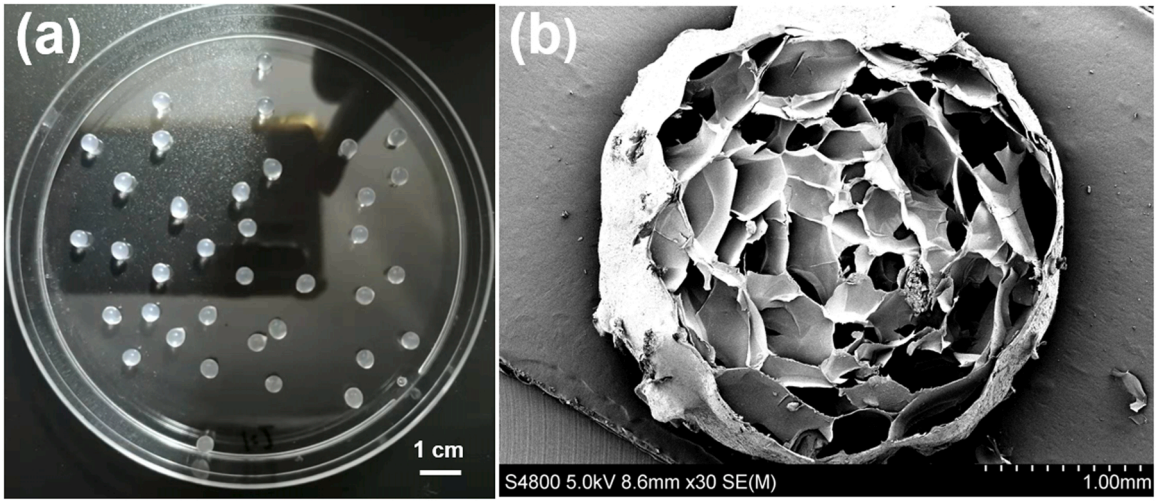

Fig. 1. (a) Digital photo and (b) electron microscopy image of bead prepared with gelatin-to-sodium alginate ratio 1:2.

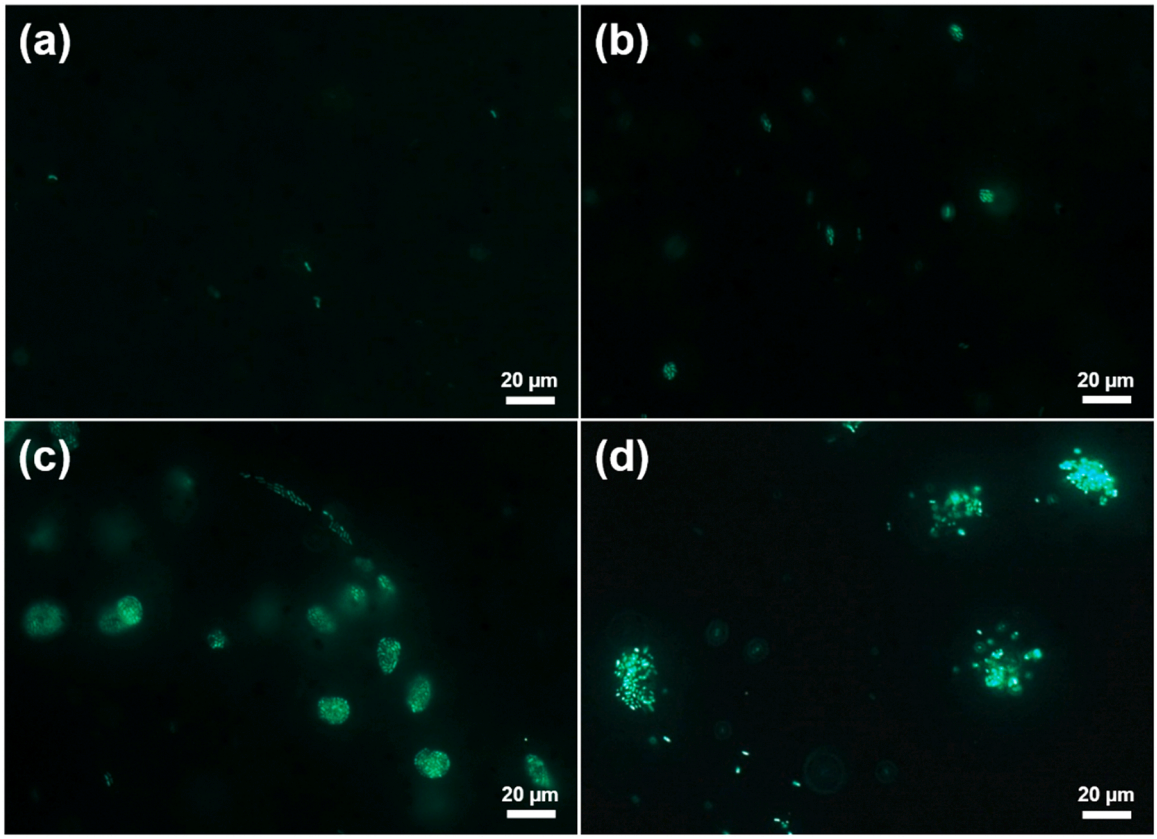

Fig. 2. Fluorescence micrographs of the HP-7 strain in bio-beads at different growth times. (a) 0 h, (b) 6 h, (c) 12 h, and (d) 24 h.

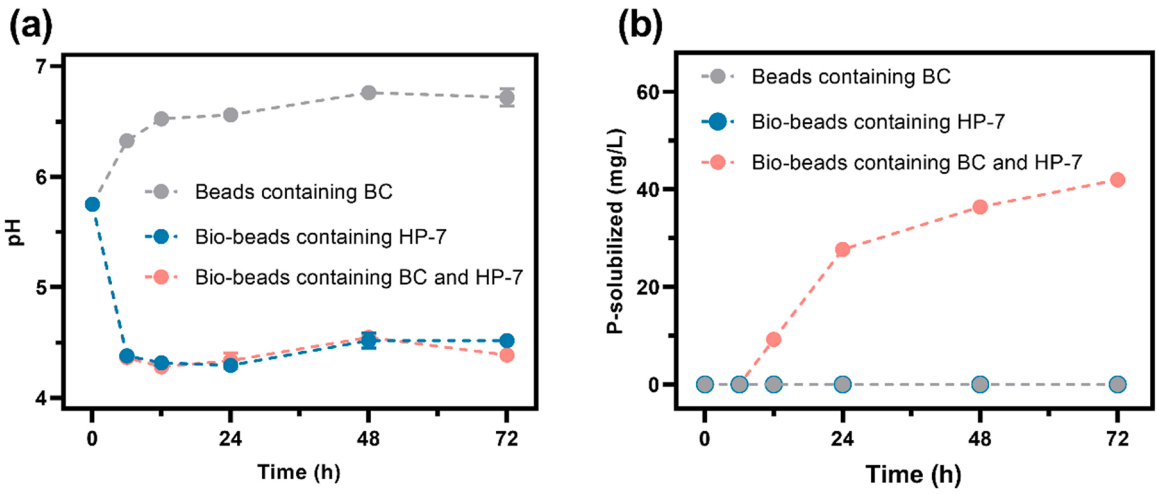

Fig. 3. Release of P in bio-beads in the presence of the HP-7 strain. Changes in (a) pH and (b) soluble P concentration with time. (BC in the figures refer to bone char).

strain encapsulated inside the bio-beads still had the ability to dissolve and release P into the solution from the bone char encapsulated inside the bio-beads.

3.4. Pb^{2+} removal performance of bio-beads

Fig. 4 shows the removal efficiency of Pb^{2+} under different treatments. In the control check, the residual Pb^{2+} concentration was 182.1 mg/L. Compared with the control check, the residual Pb^{2+} concentration slightly increased in the group with the addition of free bacteria. This may result from the rupture of the strain and binding of intracellular material to the insoluble state of Pb, which increased the concentration of soluble Pb^{2+}. The Pb^{2+} removal efficiency of the bio-beads containing only the HP-7 strain was 51.7 %. The number of bacteria encapsulated in the bio-beads was the same as that of the free bacteria. Bacteria have a lower adsorption capacity for Pb^{2+}, indicating that alginate and gelatin are the main contributors to the removal of Pb^{2+} by the bio-bead containing only the HP-7 strain. Alginate and gelatin absorb part of the Pb^{2+}, which reduces the toxicity of Pb^{2+} to the HP-7 strain within the bio-bead. The Pb^{2+} removal efficiency of beads containing only bone char was 72.7 %. In addition to the adsorption of alginate and gelatin, hydroxyapatite (the main component of bone char) is also a good adsorbent. Pb^{2+} can replace Ca^{2+} in hydroxyapatite through ion exchange. In addition, Pb^{2+} in solution easily forms Pb

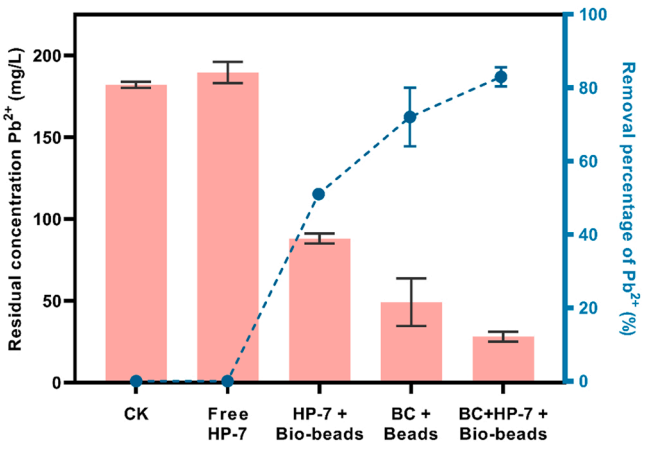

Fig. 4. Removal efficiency of Pb(II) under different treatments.

$(OH)_2$ when the pH is greater than 6. Therefore, Pb^{2+} removal experiments are usually performed in solutions with pH lower than 6. In this study, after adding Pb^{2+}, the pH of the solution was 5.1. Under acidic conditions, hydroxyapatite also dissolves and releases phosphate to react with Pb^{2+}. The removal efficiency of Pb^{2+} in the bio-bead containing bone char and the HP-7 strain increased to 83.5 %. This was because the metabolic activity of the HP-7 strain further reduced the pH to 4.6. A lower pH value further promotes the dissolution of hydroxyapatite, releasing phosphate ions, and reacting with Pb^{2+} to form a precipitate [4]. He et al. [27] found that *Phanerochaete chrysosporium* can similarly promote hydroxyapatite dissolution by secreting organic acids. The released phosphate reacts with Pb^{2+} to form Pb-phosphate compounds, thus enhancing the removal efficiency of Pb^{2+}. The changes in the solution and bio-beads before and after the reaction with Pb^{2+} are shown in Fig. S4. No large amounts of precipitation were observed in the solution before and after the reaction with Pb^{2+} (Fig. S4b). After reacting with Pb^{2+}, many white spots formed on the surface of the bio-beads (Fig. S4d). This may indicate that most of the Pb^{2+} was first adsorbed on the bio-bead surface, and then the phosphate released by the HP-7 strain from the bone char combined with the adsorbed Pb^{2+} to form Pb-phosphate compounds on the bio-bead surface.

Fig. 5a shows the effects of bone char content in the bio-beads on Pb^{2+} removal. When the bone char content increased to 6 g/L, the residual Pb^{2+} concentration decreased to 0.6 mg/L (Pb^{2+} removal efficiency reached 99.4 %, as shown in Fig. S5a) and the residual dissolved P content was 1.5 mg/L. Continuing to increase the bone char content also increased the residual dissolved P content to 2.6 mg/L. Excessive dissolved P not only increases the cost of remediation but also leads to the eutrophication of the water body [8]. Therefore, 6 g/L of bone char was chosen for subsequent experiments. Fig. 5b shows the effects of bio-beads dose on Pb^{2+} removal. As can be seen in the figure, the residual Pb^{2+} concentration decreased and amount of residual dissolved P increased as the dose of bio-beads increased. At a bio-beads dose of 1.0 %, the residual Pb^{2+} concentration decreased to 0 mg/L (Pb^{2+} removal efficiency reached 100 %) and the residual soluble P concentration was 0.9 mg/L. On further increasing the bio-beads dose, the Pb^{2+} removal efficiency continued to remain at 100 % and the residual soluble P content increase to a maximum of 6.5 mg/L. Therefore, a bio-beads dose of 1.0 % was chosen for subsequent experiments. The concentration of Pb^{2+} has an important influence on the Pb^{2+} removal efficiency. In the present work, Pb^{2+} removal efficiency by bio-beads at different initial concentrations (0.05−3 mM) were investigated (Fig. 5c). At initial concentrations of 0.05 mM, 0.5 mM, and 1 mM, the removal efficiencies were 100 %, 100 %, and 99.5 %, respectively. With continued increase

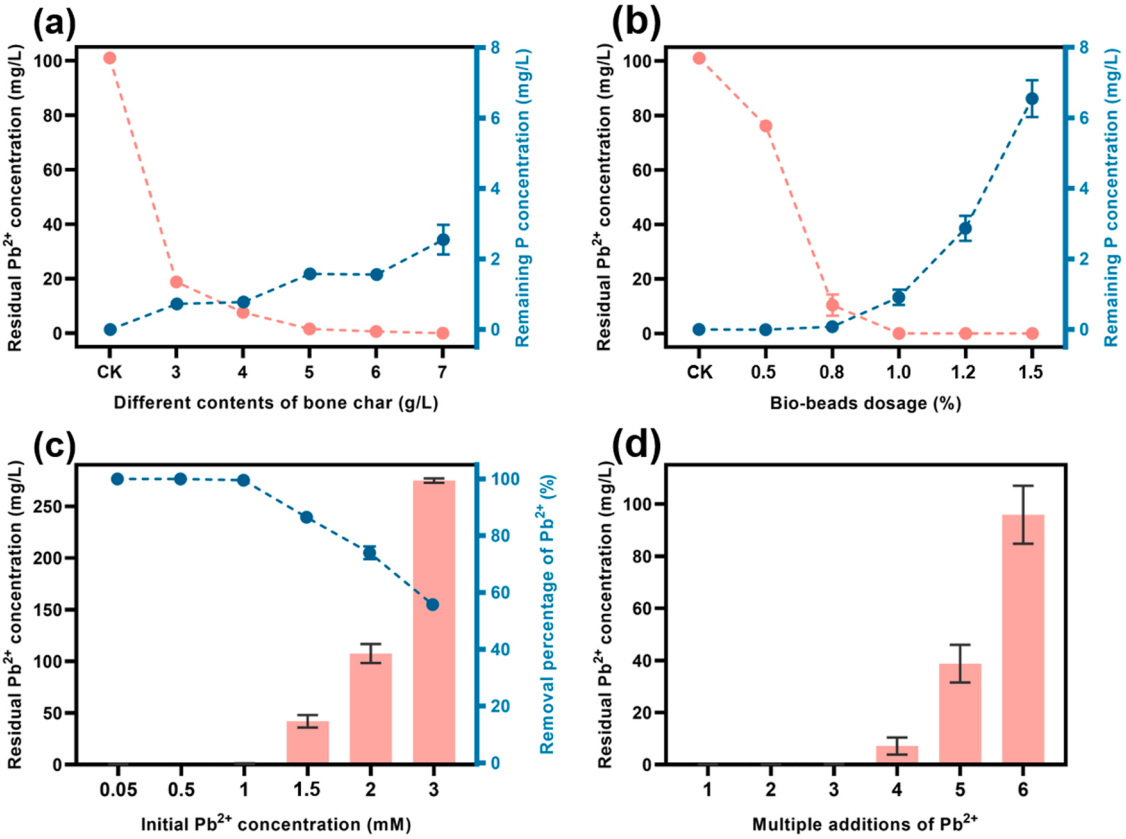

Fig. 5. Effects of (a) bone char content, (b) bio-beads dosage, (c) initial Pb^{2+} concentration, and (d) multiple Pb^{2+} additions on Pb^{2+} removal (50 mg/L Pb^{2+} per addition).

in the initial Pb^{2+} concentration, the removal efficiency of the bio-beads for Pb^{2+} decreased significantly. This may be due to two reasons. On the one hand, as the initial Pb^{2+} concentration increased, it inhibited the metabolic activity of the phosphate-solubilizing bacteria; on the other hand, the P content of the bone char in the bio-beads was not sufficient to immobilize the high concentration of Pb^{2+}. To verify the long-term stability of the bio-beads, 50 mg/L Pb^{2+} was added to the solution every 2 days. The concentration of residual Pb^{2+} in the solution is shown in Fig. 5d. After the first three additions of Pb^{2+}, no residual dissolved Pb^{2+} was detected in the solution; after the fourth, fifth, and sixth additions of Pb^{2+}, the concentrations of the remaining Pb^{2+} were 7.1, 38.8, and 95.9 mg/L, respectively. This may be because the P in the bone char in the bio-beads was sufficient during the first three additions of Pb^{2+}; after the fourth addition, the P in the bone char in bio-beads was depleted, thus leaving residual Pb^{2+} in the solution.

As shown in Table 1, the bio-beads synthesized in the present study using alginate and gelatin with encapsulated *P. rhodesiae* HP-7 and bone char exhibited high Pb^{2+} removal efficiency compared to that of other materials in previous studies. Bone char, made from waste animal bones, can replace phosphate minerals such as $Ca_3(PO_4)_2$ or $Ca_{10}(PO_4)_6(OH)_2$ as P sources. In the presence of the HP-7 strain, P within the bone char can be released to immobilize Pb. This is important for both resource utilization of waste and remediation of Pb contamination.

3.5. Characterization of bio-beads

The morphological changes on the surface and inside the bio-beads before and after the reaction with Pb^{2+} were observed using SEM. Fig. 6a shows that, before the reaction with Pb^{2+}, the bio-bead surface was flat and had strains adhering to it. Fig. S6b shows the EDS spectra of the bio-bead surface before the reaction with Pb^{2+}. The main elements are C, O, Ca, P, and Cl. Fig. 6b shows the morphology of the bio-bead surface after the reaction with Pb^{2+}. Folds appeared on the bio-bead surface, along with a large amount of granular material. In addition, the strains that adhered to the bio-bead surface disappeared, probably because the high concentration of Pb^{2+} caused the strains on the surface of the bio-beads to break up, die, and fall off [1]. Fig. S6d shows the EDS spectra of the bio-bead surface after the reaction with Pb^{2+}. As can be seen in the figure, the main elements were Pb, Cl, P, C, and O. Comparing Fig. S6d and S6b, it was found that the characteristic peak of Ca on the bio-bead surface disappeared and a new characteristic peak of Pb appeared. This results from the gradual dissolution of bone char in the presence of the HP-7 strain and the gradual release of Ca and P into the solution [4]. In contrast, Pb^{2+} diffused from the solution to the bio-bead surface and was adsorbed by the bio-beads or immobilized by phosphate. Fig. 6c and 6d show the morphology of the bio-bead inner before and after the reaction with Pb^{2+}. The presence of these strains can be observed in both figures. Fig. S6h shows the EDS spectra of the bio-beads after reaction with Pb^{2+}. The main elements inside the bio-beads were Pb, P, Cl, C, and O. This indicates that Pb^{2+} diffused not only from the solution to the surface of the bio-beads but also through the bio-bead surface and into its interior.

FT-IR characterization was performed to determine the changes in the functional groups of the bio-bead components before and after reaction with Pb^{2+} (Fig. 7). Alginate exhibited characteristic peaks at 1605.33 cm^{-1} and 1421.01 cm^{-1} owing to asymmetric and symmetric stretching vibrations of C=O in the carboxyl group (Fig. 7a); these two peaks shifted to 1588.87 cm^{-1} and 1412.85 cm^{-1} after reaction with Pb^{2+}, indicating the involvement of the carboxyl group in the adsorption of Pb^{2+} [29]. The peak shifted from 1030.64 cm^{-1} to 1026.45 cm^{-1}, implying the binding of hydroxyl groups and Pb^{2+} [30]. In the alginate and gelatin samples, carboxyl and hydroxyl groups were the main functional groups involved in the adsorption of Pb^{2+}. Fig. 7b shows the changes in the HP-7 strain and bone char before and after reaction with Pb^{2+}. The absorption peaks of the HP-7 strain at 1541.39 cm^{-1} and 1080.91 cm^{-1} were attributed to the stretching vibration of the −NH and $-PO_4^{3-}$ functional groups, respectively; the peaks shifted to 1539.12 cm^{-1} and 1078.21 cm^{-1} upon adsorption of Pb^{2+} [31,32]. In contrast, the intensity of the characteristic peak of the C−O functional group at 1384.46 cm^{-1} was significantly lower, indicating that the C−O bond on the strain surface was also involved in the adsorption of Pb^{2+}. Teng et al. investigated the mechanism of Pb^{2+} removal by *L. adecarboxylata*. The results showed that the carboxyl, hydroxyl, and amino functional groups in the extracellular polymer secreted by bacteria removed Pb^{2+} through complexation [33]. The characteristic peaks at 1640.43 cm^{-1} and 1469.07 cm^{-1} for the bone char sample correspond to the stretching vibrations of the aromatic C=C/C=O and aromatic C=O bonds [20]. The absorption peaks at 1038.04 cm^{-1} are attributed to the stretching vibration of ν_3 P−O. The peaks at 961.38 cm^{-1}, 604.11 cm^{-1} and 564.51 cm^{-1} correspond to the bending vibration of ν_2 O−P−O and ν_4 O−P−O, respectively [20]. After reaction with Pb^{2+}, the peak at 1640.43 cm^{-1} (C=C and C=O) shifted to 1647.09 cm^{-1}. The characteristic peaks of −COO (1469.07 cm^{-1}), −OH (1448.70 cm^{-1}), and the phosphate group (1038.04 cm^{-1}) shifted after the adsorption of Pb^{2+}. These results suggest that carboxyl, hydroxyl, and phosphate groups in bone char are involved in binding to Pb^{2+}.

To determine the types of Pb compounds formed after the reaction, the bio-bead samples before and after reaction with Pb were characterized using XRD (Fig. 8). No new diffraction peaks were observed before and after the reaction with Pb^{2+} for the bio-beads alone or for the bio-beads containing the HP-7 strain. The characteristic peaks of hydroxyapatite could be seen in the bio-beads containing bone char before the reaction with Pb^{2+} because the main component of bone char is hydroxyapatite. After reaction with Pb^{2+}, the characteristic peak of $Pb_5(PO_4)_3Cl$ was observed because, under weakly acidic conditions (pH 5.1), the bone char slowly dissolved and the released phosphate that reacted with Pb^{2+} to form $Pb_5(PO_4)_3Cl$. The characteristic peak of bone char was also detected in the bio-beads containing both bone char and phosphate-solubilizing bacteria before reaction with Pb^{2+}. After reaction with Pb^{2+}, the characteristic peak of bone char disappeared, and a new peak of $Pb_5(PO_4)_3Cl$ appeared. The metabolic activity of the HP-7 strain in the bio-beads resulted in a lower pH (4.6), which facilitated the release of phosphate from the bone char, thus allowing Pb^{2+} to be transformed into $Pb_5(PO_4)_3Cl$.

To characterize the activity of phosphate-solubilizing bacteria after reaction with Pb^{2+}, the HP-7 strain was observed using fluorescence

Table 1
Comparison of Pb^{2+} removal efficiency of bio-beads in this study with that reported in previous studies.

Materials	Phosphorus source	pH	Initial concentration of Pb^{2+} ((mg/L)	Time (h)	Pb^{2+} removal efficiency (%)	Ref.
PSB capsules[a]	$Ca_3(PO_4)_2$	3.0	140	24	98.4	[8]
PSB beads[b]	$Ca_3(PO_4)_2$ or beef peptone medium	5.0	200	24	93	[23]
PSB microcapsules[c]	$Ca_{10}(PO_4)_6(OH)_2$	6.0	100	144	89.67	[27]
PSB beads[d]	bone char	5.1	200	72	100	This study

[a] Capsules formed by alginate encapsulated *L. adecarboxylata* L15 and $Ca_3(PO_4)_2$.
[b] Bio-beads of polyvinyl alcohol and alginate encapsulated with *L. adecarboxylata* L15 and biochar loaded with zero-valent iron nanoparticles.
[c] Microcapsules formed by alginate encapsulated *Phanerochaete chrysosporium* and hydroxyapatite.
[d] Bio-beads of alginate and gelatin encapsulated with *P. rhodesiae* HP-7 and bone char.

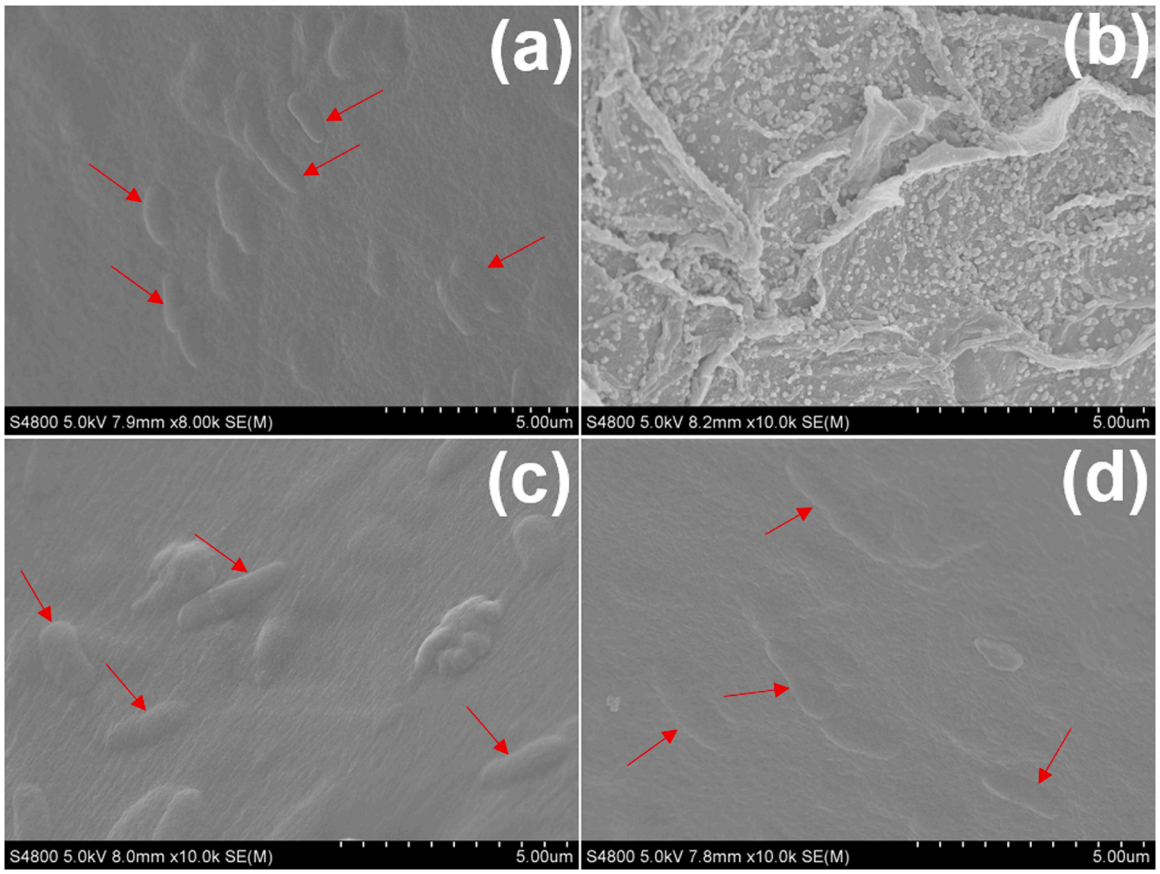

Fig. 6. SEM images of bio-beads containing the HP-7 strain and bone char: Surface of bio-beads (a) before and (b) after reacting with Pb(II). Inner region of bio-beads (c) before and (d) after reacting with Pb(II).

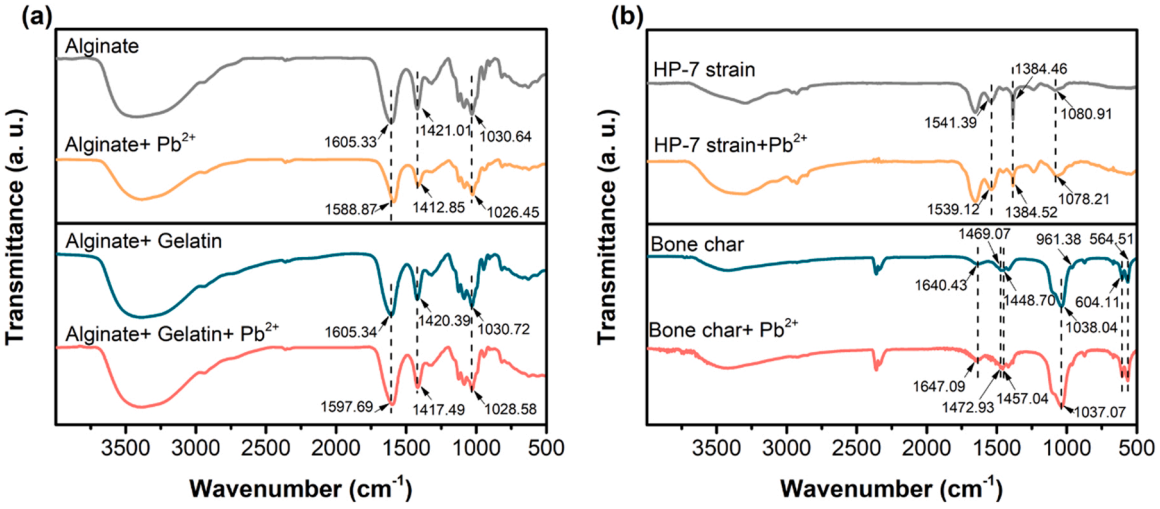

Fig. 7. FT-IR spectra of bio-bead components before and after reaction with Pb^{2+}. (a) Alginate, alginate and gelatin; (b) HP-7 strain and bone char.

microscopy after staining with STYO9/PI. STYO9 stains both dead and live bacteria and they emit green fluorescence, whereas PI stains only dead bacteria which emit red fluorescence. As shown in Fig. S7a and S7b, after reaction of the free strain with 1 mM Pb^{2+}, most of the strain showed red fluorescence, indicating lysis of the strain. When only the HP-7 strain was encapsulated (Fig. S7c and S7d), some HP-7 strains died, indicating that Pb^{2+} that entered the interior of the bio-beads was still toxic to the HP-7 strain. The encapsulation of both the HP-7 strain and bone char (Fig. S7e and S7f) resulted in the death of only a small number of strains. This result suggests that encapsulation can improve the resistance of the HP-7 strain to high concentrations of Pb^{2+} (1 mM).

3.6. *Mechanism of Pb^{2+} removal using bio-beads*

Based on the above characterization results, two types of mechanisms for the removal of Pb^{2+} using bio-beads were proposed. The first of these is adsorption. Pb^{2+} in the solution reached the surface of the bio-beads by diffusion. The hydroxyl and carboxyl groups in alginate and

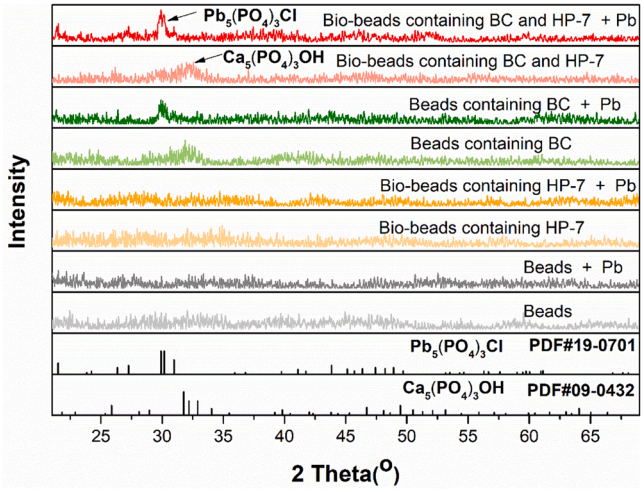

Fig. 8. XRD patterns of different beads before and after reaction with Pb^{2+}.

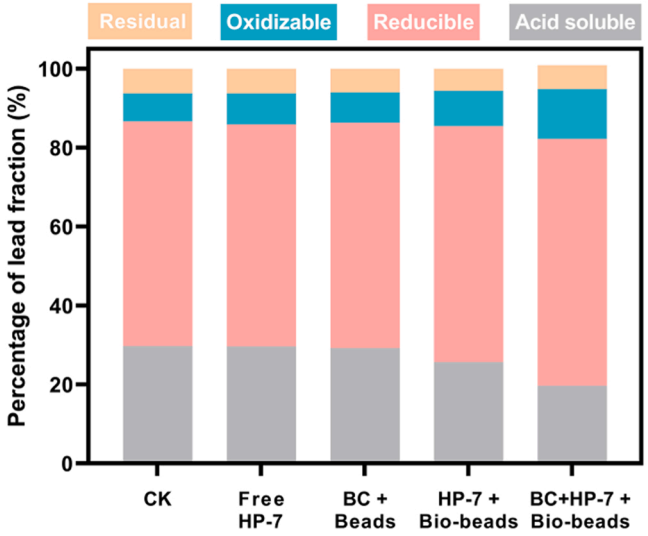

Fig. 9. Percentage of lead fractions in soil after 10 days of remediation with control check, free HP-7 strain, beads containing bone char, bio-beads containing HP-7 strain, and bio-beads containing bone char and HP-7 strain.

gelatin on the surface of the bio-beads bind to Pb^{2+} and adsorb some of them to the surface of the bio-beads. As Pb^{2+} diffused further into the bio-beads, the bone char and *P. rhodesiae* strain were able to adsorb Pb^{2+}. The hydroxyl, carboxyl, and phosphate groups in bone char and the C–O bond, –NH, and $–PO_4^{3-}$ functional groups of the bacteria are involved in Pb^{2+} binding. The second removal mechanism involved mineralization, which can be subdivided into two types. 1) Chemical substitution reactions, where Pb^{2+} can replace Ca^{2+} in $Ca_5(PO_4)_3OH$ (hydroxyapatite, the main component of bone char), whereas Cl^- in solution can replace OH^-, resulting in the formation of $Pb_5(PO_4)_3Cl$. 2) A dissolution-precipitation mechanism involving the HP-7 strain, where organic acids produced by *P. rhodesiae* HP-7 lower the pH of the solution, thus allowing hydroxyapatite in bone char to dissolve and release phosphate. Phosphate combines with Pb^{2+} to form $Pb_5(PO_4)_3Cl$ precipitate. Dissolution precipitation has been shown to be the dominant mechanism for the formation of $Pb_5(PO_4)_3Cl$ compared to substitution reactions [28,34]. Thus, *P. rhodesiae* HP-7 plays an important role in the immobilization of Pb^{2+} by bone char.

3.7. Remediation of lead-containing soils by bio-beads

The results of lead passivation in the soil by control check (CK), free HP-7 strain, beads containing bone char, bio-beads containing HP-7 strain, and bio-beads containing HP-7 strain and bone char are shown in Fig. 9. The acid-soluble fraction of Pb in the original soil was 29.8 %. Among all the treatments, the bio-beads containing both bone char and the HP-7 strain showed the best remediation efficiency after 10 days of remediation. Compared to the control check, the acid-soluble fraction decreased from 29.8 % to 19.7 % (a 34 % reduction), the reducible fraction increased from 56.8 % to 60.9 %, and the oxidizable fraction increased from 7.1 % to 11.5 %. This indicates that the bio-beads containing both bone char and the HP-7 strain transformed the unstable acid-soluble fraction into reducible and oxidizable fractions. The fraction transformation may result from the adsorption and precipitation of lead from phosphate released by the HP-7 strain from bone char or soil to form a relatively stable lead-containing phosphate. Similarly, Zhao et al. [35] found that phosphate-solubilizing bacteria dissolved biochar-supported nano-hydroxyapatite (nHAP@biochar) to release soluble P, thereby converting the acid-soluble fraction Cd in the soil to reducible, oxidizable, and residual fractions of Cd. The acid-soluble fractions in soil treated with free HP-7 strain, beads containing only bone char, and bio-beads containing only HP-7 strain were reduced to only 29.7 %, 29.2 %, and 25.7 %, respectively. In soil remediation, the beads containing only bone char exhibited essentially no lead immobilization, which was completely different from Pb^{2+} removal in solution (Fig. 4). Possible reasons include: 1) Pb in the soil was insoluble and the bone char within the beads was unable to immobilize insoluble lead by adsorption or substitution reactions; 2) the pH of the soil solution was 8.0, which is different from the acidic conditions (pH 5.1) of the Pb^{2+} removal experiments. Under alkaline conditions and in the absence of the HP-7 strain, bone char could not dissolve and release phosphate to immobilize lead. The results of the soil remediation experiments also demonstrated the important role of the HP-7 strain and the effectiveness and superiority of the combined bio-beads. To verify the long-term stability of the bio-beads in flooded soil, we extended the remediation experiments to 30 d. After 30 d, the bio-beads were removed from the soil, and the shape of the bio-beads is shown in Fig. S8. The bio-beads of all groups still maintained their spherical shape. This indicates that the bio-beads formed from alginate and gelatin in this study have good long-term stability.

To observe the survival of the strain inside bio-beads after 30 d of remediation of Pb-contaminated soil, we used a laser confocal microscope to observe dead and live cells in 3D (Fig. 10 and S9). The 3D photographs of bio-beads containing only the HP-7 strain and bio-beads containing both the HP-7 strain and bone char after 30 d of remediation of lead-contaminated soil are shown in Fig. 10a and b. Most bacteria in the bio-beads showed green fluorescence, indicating that the vast majority of the cells in the bio-beads were viable. The statistical results for the number of live bacteria inside the bio-beads on day 0 (Figs. S9a or S9b) and day 30 (Fig. 10a or b) are shown in Fig. 10c. There was a significant increase in the number of bacteria inside the bio-beads after 30 d compared with that on day 0. This indicated that alginate and gelatin provided a suitable environment for the growth of the HP-7 strain. Compared with the number of live bacteria in the bio-beads containing only the HP-7 strain and those containing both the HP-7 strain and bone char on day 30, the addition of bone char significantly increased the number of HP-7 bacteria. This is because the metabolism of the HP-7 strain can dissolve bone char and release phosphate. On the one hand, it provides an additional P source for the growth of the HP-7 strain; on the other hand, phosphate reduces the bioavailability of Pb in soil (Fig. 9), thus reducing toxicity to the HP-7 strain. The above results showed that the bio-beads made of alginate and gelatin-embedded HP-7 strain and bone char had good stability and could be used to remediate Pb-polluted environments.

The bio-beads proposed in this study showed good lead immobilization performance in both solution and soil. However, some factors must be considered when applying them in a real environment, such as

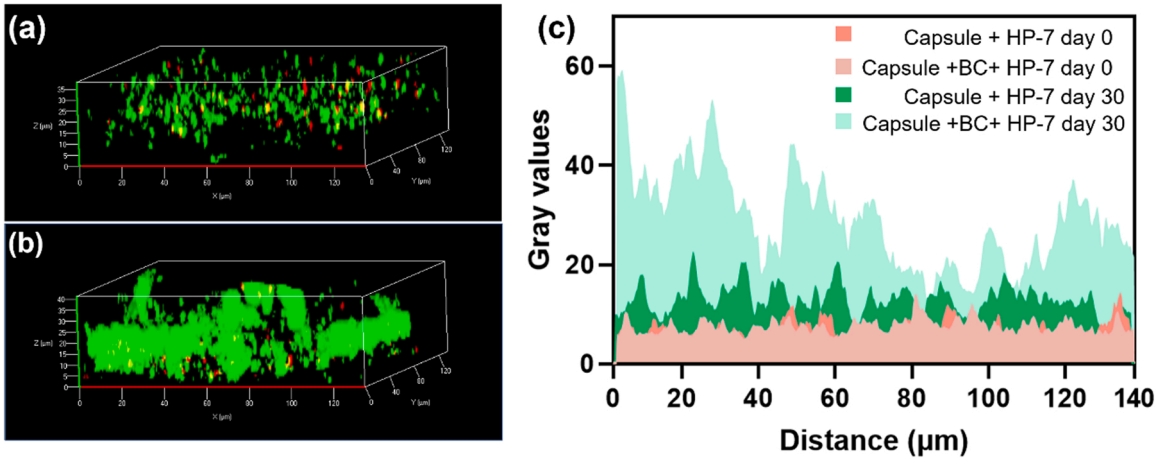

Fig. 10. Three-dimensional laser confocal microscopy images of (a) bio-beads containing only the HP-7 strain and (b) bio-beads containing both the HP-7 strain and bone char after 30 d of remediation of lead-contaminated soil; (c) Statistical graph of the number of live bacteria in the bio-beads.

the limitations of carbon and nitrogen sources and the water content of the soil. In reality, carbon and nitrogen sources may be too low for the growth of phosphate-solubilizing bacteria. When sufficient carbon and nitrogen sources are added directly to the environment, it can easily lead to environmental eutrophication. Future work should consider encapsulating the carbon and nitrogen sources required for microbial growth in bio-beads. The water content of the soil is also a key factor. In this study, flooded soil was used in the soil remediation experiments to allow nutrients to enter the interior of the bio-beads and P from bone char to be released from the interior of the bio-beads to the soil environment. The bio-beads prepared in this study are more suitable for the remediation of soils with high water content, such as sediments and paddy soils.

4. Conclusion

In the present study, bio-beads containing the HP-7 strain and bone char were constructed using sodium alginate and gelatin. The ability of the HP-7 strain to release P from bone char, the immobilization mechanism of Pb by bio-beads, and the long-term stability of bio-beads were investigated. The results showed that bone char released phosphate in the presence of the HP-7 strain. Most Pb^{2+} was immobilized on the surface of bio-beads through the formation of $Pb_5(PO_4)_3Cl$. The acid-soluble fraction of Pb in the soil was transformed into reducible and oxidizable fractions. The bio-beads showed good stability after up to 30 d of soil remediation, and the HP-7 strain inside the bio-beads grew normally. The present study shows that bone char can be transformed into a low-cost and efficient Pb immobilization material by the action of phosphate-solubilizing bacteria; the bio-beads containing the HP-7 strain and bone char have the potential to remediate Pb-contaminated environments.

CRediT authorship contribution statement

Junpeng Li: Conceptualization, Methodology, Investigation, Writing—original draft preparation, Writing—review and editing; **Rui Bai:** Investigation, Writing—original draft preparation, Visualization; **Wei Chen:** Investigation, Visualization; **Chongyuan Ren:** Investigation, Visualization; **Fan Yang:** Methodology, Investigation; **Xiaochun Tian:** Methodology, Investigation; **Xiaofeng Xiao:** Investigation, Visualization; **Feng Zhao:** Conceptualization, Writing—review and editing, Supervision, Project administration, Funding acquisition. All authors have read and agreed to the published version of the manuscript.

Declaration of Competing Interest

The authors declare that they have no known competing financial interests or personal relationships that could have appeared to influence the work reported in this paper.

Data availability

No data was used for the research described in the article.

Acknowledgements

This work was supported by the National Natural Science Foundation of China (No. 42021005 and 22236007) and the National Key R&D Program of China (2018YFC1800502).

Appendix A. Supporting information

Supplementary data associated with this article can be found in the online version at doi:10.1016/j.jhazmat.2023.130772.

References

[1] Chen, Z., Pan, X., Chen, H., Guan, X., Lin, Z., 2016. Biomineralization of Pb(II) into Pb-hydroxyapatite induced by *Bacillus cereus* 12-2 isolated from lead-zinc mine tailings. J Hazard Mater 301, 531–537. https://doi.org/10.1016/j.jhazmat.2015.09.023.

[2] Zeng, G., Wan, J., Huang, D., Hu, L., Huang, C., Cheng, M., Xue, W., Gong, X., Wang, R., Jiang, D., 2017. Precipitation, adsorption and rhizosphere effect: the mechanisms for Phosphate-induced Pb immobilization in soils-a review. J Hazard Mater 339, 354–367. https://doi.org/10.1016/j.jhazmat.2017.05.038.

[3] Miretzky, P., Fernandez-Cirelli, A., 2008. Phosphates for Pb immobilization in soils: a review. Environ Chem Lett 6, 121–133. https://doi.org/10.1007/s10311-007-0133-y.

[4] Li, J., Tian, X., Bai, R., Xiao, X., Yang, F., Zhao, F., 2022. Transforming cerussite to pyromorphite by immobilising Pb(II) using hydroxyapatite and *Pseudomonas rhodesiae*. Chemosphere 287, 132235. https://doi.org/10.1016/j.chemosphere.2021.132235.

[5] Li, Z., Wang, F., Bai, T., Tao, J., Guo, J., Yang, M., Wang, S., Hu, S., 2016. Lead immobilization by geological fluorapatite and fungus *Aspergillus niger*. J Hazard Mater 320, 386–392. https://doi.org/10.1016/j.jhazmat.2016.08.051.

[6] Teng, Z., Shao, W., Zhang, K., Huo, Y., Li, M., 2019. Characterization of phosphate solubilizing bacteria isolated from heavy metal contaminated soils and their potential for lead immobilization. J Environ Manag 231, 189–197. https://doi.org/10.1016/j.jenvman.2018.10.012.

[7] Xu, J.C., Huang, L.M., Chen, C., Wang, J., Long, X.X., 2019. Effective lead immobilization by phosphate rock solubilization mediated by phosphate rock amendment and phosphate solubilizing bacteria. Chemosphere 237, 124540. https://doi.org/10.1016/j.chemosphere.2019.124540.

[8] Zhang, K., Teng, Z., Shao, W., Wang, Y., Li, M., Lam, S.S., 2020. Effective passivation of lead by phosphate solubilizing bacteria capsules containing

tricalcium phosphate. J Hazard Mater 397, 122754. https://doi.org/10.1016/j.jhazmat.2020.122754.
[9] Glaesner, N., Hansen, H.C.B., Hu, Y., Bekiaris, G., Bruun, S., 2019. Low crystalline apatite in bone char produced at low temperature ameliorates phosphorus-deficient soils. Chemosphere 223, 723–730. https://doi.org/10.1016/j.chemosphere.2019.02.048.
[10] Qian, T., Yang, Q., Jun, D.C.F., Dong, F., Zhou, Y., 2019. Transformation of phosphorus in sewage sludge biochar mediated by a phosphate-solubilizing microorganism. Chem Eng J 359, 1573–1580. https://doi.org/10.1016/j.cej.2018.11.015.
[11] Azeem, M., Shaheen, S.M., Ali, A., Jeyasundar, P., Latif, A., Abdelrahman, H., Li, R., Almazroui, M., Niazi, N.K., Sarmah, A.K., Li, G., Rinklebe, J., Zhu, Y.G., Zhang, Z., 2022. Removal of potentially toxic elements from contaminated soil and water using bone char compared to plant- and bone-derived biochars: a review. J Hazard Mater 427, 128131. https://doi.org/10.1016/j.jhazmat.2021.128131.
[12] Li, H., Li, Y., Xu, Y., Lu, X., 2020. Biochar phosphorus fertilizer effects on soil phosphorus availability. Chemosphere 244, 125471. https://doi.org/10.1016/j.chemosphere.2019.125471.
[13] Peng, Y., Azeem, M., Li, R., Xing, L., Li, Y., Zhang, Y., Guo, Z., Wang, Q., Ngo, H.H., Qu, G., Zhang, Z., 2022. Zirconium hydroxide nanoparticle encapsulated magnetic biochar composite derived from rice residue: application for As(III) and As(V) polluted water purification. J Hazard Mater 423, 127081. https://doi.org/10.1016/j.jhazmat.2021.127081.
[14] Wu, W., Liu, Z., Azeem, M., Guo, Z., Li, R., Li, Y., Peng, Y., Ali, E.F., Wang, H., Wang, S., Rinklebe, J., Shaheen, S.M., Zhang, Z., 2022. Hydroxyapatite tailored hierarchical porous biochar composite immobilized Cd(II) and Pb(II) and mitigated their hazardous effects in contaminated water and soil. J Hazard Mater 437, 129330. https://doi.org/10.1016/j.jhazmat.2022.129330.
[15] Li, Y., Shaheen, S.M., Azeem, M., Zhang, L., Feng, C., Peng, J., Qi, W., Liu, J., Luo, Y., Peng, Y., Ali, E.F., Smith, K., Rinklebe, J., Zhang, Z., Li, R., 2022. Removal of lead (Pb^{+2}) from contaminated water using a novel MoO_3-biochar composite: performance and mechanism. Environ Pollut 308, 119693. https://doi.org/10.1016/j.envpol.2022.119693.
[16] Ren, J., Zhao, Z., Ali, A., Guan, W., Xiao, R., Wang, J.J., Ma, S., Guo, D., Zhou, B., Zhang, Z., Li, R., 2019. Characterization of phosphorus engineered biochar and its impact on immobilization of Cd and Pb from smelting contaminated soils. J Soils Sediment 20, 3041–3052. https://doi.org/10.1007/s11368-019-02403-6.
[17] Reynel-Avila, H.E., Mendoza-Castillo, D.I., Bonilla-Petriciolet, A., 2016. Relevance of anionic dye properties on water decolorization performance using bone char: adsorption kinetics, isotherms and breakthrough curves. J Mol Liq 219, 425–434. https://doi.org/10.1016/j.molliq.2016.03.051.
[18] Wang, M., Liu, Y., Yao, Y., Han, L., Liu, X., 2020. Comparative evaluation of bone chars derived from bovine parts: physicochemical properties and copper sorption behavior. Sci Total Environ 700, 134470. https://doi.org/10.1016/j.scitotenv.2019.134470.
[19] Liu, Y., Xu, J., Cao, Z., Fu, R., Zhou, C., Wang, Z., Xu, X., 2020. Adsorption behavior and mechanism of Pb(II) and complex Cu(II) species by biowaste-derived char with amino functionalization. J Colloid Interface Sci 559, 215–225. https://doi.org/10.1016/j.jcis.2019.10.035.
[20] Xiao, J., Hu, R., Chen, G., 2020. Micro-nano-engineered nitrogenous bone biochar developed with a ball-milling technique for high-efficiency removal of aquatic Cd (II), Cu(II) and Pb(II). J Hazard Mater 387, 121980. https://doi.org/10.1016/j.jhazmat.2019.121980.
[21] Chen, H., Zhang, J., Tang, L., Su, M., Tian, D., Zhang, L., Li, Z., Hu, S., 2019. Enhanced Pb immobilization via the combination of biochar and phosphate solubilizing bacteria. Environ Int 127, 395–401. https://doi.org/10.1016/j.envint.2019.03.068.
[22] Tang, L., Shen, Z., Duan, X., Wang, Z., Wu, Y., Shao, X., Song, X., Hu, S., Li, Z., 2019. Evaluating the potential of charred bone as P hotspot assisted by phosphate-solubilizing bacteria. Sci Total Environ 696, 133965. https://doi.org/10.1016/j.scitotenv.2019.133965.
[23] Teng, Z., Shao, W., Zhang, K., Yu, F., Huo, Y., Li, M., 2020. Enhanced passivation of lead with immobilized phosphate solubilizing bacteria beads loaded with biochar/nanoscale zero valent iron composite. J Hazard Mater 384, 121505. https://doi.org/10.1016/j.jhazmat.2019.121505.
[24] Tu, Z., Ren, X., Zhao, J., Awasthi, S.K., Wang, Q., Awasthi, M.K., Zhang, Z., Li, R., 2019. Synergistic effects of biochar/microbial inoculation on the enhancement of pig manure composting. Biochar 1, 127–137. https://doi.org/10.1007/s42773-019-00003-8.
[25] Bu, Y., Xu, H.X., Li, X., Xu, W.J., Yin, Y.X., Dai, H.L., Wang, X.B., Huang, Z.J., Xu, P. H., 2018. A conductive sodium alginate and carboxymethyl chitosan hydrogel doped with polypyrrole for peripheral nerve regeneration. RSC Adv 8, 10806–10817. https://doi.org/10.1039/c8ra01059e.
[26] Rojek, K.O., Cwiklinska, M., Kuczak, J., Guzowski, J., 2022. Microfluidic formulation of topological hydrogels for microtissue engineering. Chem Rev. https://doi.org/10.1021/acs.chemrev.1c00798.
[27] He, N., Hu, L., He, Z., Li, M., Huang, Y., 2022. Mineralization of lead by *Phanerochaete chrysosporium* microcapsules loaded with hydroxyapatite. J Hazard Mater 422. https://doi.org/10.1016/j.jhazmat.2021.126902.
[28] Zhang, P., 1999. Transformation of Pb(II) from cerrusite to chloropyromorphite in the presence of hydroxyapatite under varying conditions of pH. Environ Sci Technol 33, 625–630. https://doi.org/10.1021/es980268e.
[29] Li, X., Qi, Y., Li, Y., Zhang, Y., He, X., Wang, Y., 2013. Novel magnetic beads based on sodium alginate gel crosslinked by zirconium(IV) and their effective removal for Pb^{2+} in aqueous solutions by using a batch and continuous systems. Bioresour Technol 142, 611–619. https://doi.org/10.1016/j.biortech.2013.05.081.
[30] Wang, F., Lu, X., Li, X.Y., 2016. Selective removals of heavy metals (Pb^{2+}, Cu^{2+}, and Cd^{2+}) from wastewater by gelation with alginate for effective metal recovery. J Hazard Mater 308, 75–83. https://doi.org/10.1016/j.jhazmat.2016.01.021.
[31] Bai, J., Yang, X., Du, R., Chen, Y., Wang, S., Qiu, R., 2014. Biosorption mechanisms involved in immobilization of soil Pb by *Bacillus subtilis* DBM in a multi-metal-contaminated soil. J Environ Sci (China) 26, 2056–2064. https://doi.org/10.1016/j.jes.2014.07.015.
[32] Zhang, K., Xue, Y., Zhang, J., Hu, X., 2020. Removal of lead from acidic wastewater by bio-mineralized bacteria with pH self-regulation. Chemosphere 241, 125041. https://doi.org/10.1016/j.chemosphere.2019.125041.
[33] Teng, Z., Shao, W., Zhang, K., Huo, Y., Zhu, J., Li, M., 2019. Pb biosorption by *Leclercia adecarboxylata*: Protective and immobilized mechanisms of extracellular polymeric substances. Chem Eng J 375. https://doi.org/10.1016/j.cej.2019.122113.
[34] Ma, Q.Y., Traina, S.J., Logan, T.J., Ryan, J.A., 1993. In-situ lead immobilization by apatite. Environ Sci Technol 27, 1803–1810. https://doi.org/10.1021/es00046a007.
[35] Zhao, X., Dai, J., Teng, Z., Yuan, J., Wang, G., Luo, W., Ji, X., Hu, W., Li, M., 2022. Immobilization of cadmium in river sediment using phosphate solubilizing bacteria coupled with biochar-supported nano-hydroxyapatite. J Clean Prod 348. https://doi.org/10.1016/j.jclepro.2022.131221.